Journal of Microscopy, Vol. 213, Pt 1 January 2004, pp. 70–75
Received 18 July 2003; accepted 4 September 2003

Fluctuation analysis of mitochondrial NADH fluorescence signals in confocal and two-photon microscopy images of living cardiac myocytes

K. BLINOVA, C. COMBS, P. KELLMAN & R. S. BALABAN
Laboratory of Cardiac Energetics, National Heart Lung and Blood Institute, National Institutes of Health, Department of Health and Human Services, Bethesda MD 20892, U.S.A.

Key words. Correlation analysis, rabbit, temperature, time series, two-photon microscopy.

Summary

A fluctuation analysis was performed on the reduced nicotine adenine dinucleotide (NADH) fluorescence signal from resting rabbit myocytes using confocal and two-photon microscopy. The purpose of this study was to establish whether any co-ordinated biochemical processes, such as binding, metabolism and inner mitochondrial membrane potential, were contributing to NADH signal fluctuations above background instrument noise. After a basic characterization of the instrument noise, time series of cellular NADH fluorescence images were collected and compared with an internal standard composed of NADH in the bathing medium. The coefficient of variation as a function of mean signal amplitude of cellular NADH fluorescence and bathing media NADH was identical even as a function of temperature. These data suggest that the fluctuations in cellular NADH fluorescence in resting myocytes are dominated by sampling noise of these instruments and not significantly modified by biological processes. Further analysis revealed no significant spatial correlations within the cell, and Fourier analysis revealed no coherent frequency information. These data suggest that the impact of biochemical processes, which might affect cellular NADH fluorescence emission, are either too small in magnitude, occurring in the wrong temporal scale or too highly spatially localized for detection using these standard optical microscopy approaches.

Introduction

As technology decreases voxel size in cellular fluorescence microscopy of naturally occurring cellular metabolites, such as NADH and reduced flavine adenine dinucleotide (FADH), the possibility of detecting local fluctuations in cellular metabolism increases. This is a result of the limited spatial averaging that will occur with small imaging voxels. Local fluctuations could provide important insights into the co-ordinated regulation of mitochondria metabolic processes within different regions of the cell as well as other metabolic processes. It has been shown by several investigators that the mitochondrial NADH or FADH fluorescence signal in confocal fluorescence microscopy of cardiac myocytes can dramatically fluctuate in highly localized regions, apparently reflecting transient metabolic events under specialized conditions (e.g. O'Rourke *et al.*, 1995; Duchen *et al.*, 1998; Romashko *et al.*, 1998). These authors either found periodic oscillations in mitochondrial FADH/NADH (O'Rourke *et al.*, 1995) or flickering of the mitochondrial membrane potential, which is linked to NADH levels (Territo *et al.*, 2000), in discrete regions in the cell (Duchen *et al.*, 1998). Thus, it is reasonable to assume that even under resting conditions biochemically linked processes could contribute to the fluctuation of the NADH or FADH signal, providing useful information on these processes.

Several factors could contribute to a biochemical source of signal fluctuation in NADH fluorescence, including changes in binding (Estabrook, 1962; Wakita *et al.*, 1995), metabolic consumption or production, diffusion or rapid changes in mitochondrial proton motive force (PMF) because the NADH redox couple is tightly linked to PMF via site 1 of oxidative phosphorylation. Owing to the high concentration of NADH in the cell and mitochondria (~3 mM in mitochondria; Klingenberg *et al.*, 1959) it is unlikely that single molecular events could be detected. As a result of this high concentration, any biological sources of NADH fluctuations would have to represent a co-ordinated NADH response within significant regions of the cell (i.e. an entire mitochondrion for example) to be detected with this approach. The most likely candidate for this type of co-ordinated fluctuation would be local variations in PMF, as described by Duchen *et al.* (1998). A local change in PMF would coordinate the ~3 mM NADH signal within a given mitochondria, resulting in a large local fluorescence modification.

Correspondence to: Dr Ksenia Blinova. E-mail: blinovak@nhlbi.nih.gov

The purpose of this study was to evaluate whether fluctuations in resting rabbit cardiac myocyte NADH fluorescence have contributions from biological processes in excess of the instrument noise. This was accomplished by comparing the fluctuations in cellular NADH signals with free NADH solutions as internal or paired controls under a variety of temperatures and conditions.

Materials and methods

Preparation of cardiac myocytes and experimental conditions

Cardiac myocytes were isolated from adult rabbits using standard procedures (Chacon *et al.*, 1994). Cells were resuspended after isolation in media consisting of a 1 : 1 mixture of Joklik's medium and medium 199 supplemented with 1 mM creatine, 1 mM carnitine, 1 mM taurine, 1 mM octanoic acid, 10 mM Hepes, 5 mM hydroxybutyric acid, 0.05 U mL^{-1} insulin, 10 U mL^{-1} penicillin and 10 μg mL^{-1} streptomycin at pH 7.4. Cells were plated onto cover slips coated with Matrigel (Becton, Dickinson, Franklin Lakes, NJ) for attachment before each experiment. All experiments were conducted within 8 h of isolation. Temperature was varied from 23 to 37 °C by controlling the air temperature in an enclosed microscope stage in addition to a Peltier device within the cell perfusion chamber.

Confocal laser scanning microscopy

Fluorescence images were obtained with a Zeiss LSM-510 confocal microscope system. Images of the isolated myocytes were collected with a C-Apochromat 63×, 1.2 NA, water lens. NADH fluorescence was imaged with the 351-nm line of a UV laser and an LP 385-nm emission filter. All image processing was performed using custom-written programs written in the IDL programming environment (RSI, Boulder, CO). Large time series of images (300–1000) were collected with the time between images varying from 30 to 500 ms. The different sampling times were used to vary the bandwidth of the fluctuation analysis. Longer time series could improve the statistical sensitivity of these measurements to biological variations; however, we reasoned that sampling times in excess of several minutes were not practical owing to cellular motion in these primary cells and non-specific effects of the laser illumination.

Two-photon laser scanning microscopy

Two-photon fluorescence images were collected using a Bio-Rad Radiance 2100 MP scanning system (Bio-Rad Laboratories, Hercules, CA) attached to a Nikon E600 FN microscope and a 60×, 1.0 NA Fluor water objective. Excitation light was provided by a 80-MHz mode-locked Ti:sapphire laser (Millenia-Tsunami combination, Spectra-Physics, Mountain View, CA). NADH fluorescence was collected in the non-descanned mode using 710-nm excitation light (Huang *et al.*, 2002) and a 450/80 emmision filter (Chroma, Brattleboro, VT). The excitation power measured at the back focal plane of the microscope did not exceed 10 mW.

Theoretical considerations

The fluctuation processes were analysed from a time series of images by estimating the probability distribution of the fluorescence intensity (i.e. histogram normalized by number of samples). Under ideal conditions, the deviation of measurements in time around their mean should follow a Possion distribution as a result of shot noise (Mandel & Wolf, 1995). This results in the variance (σ^2) equalling the mean (μ). However, other sources of noise including excitation light variation, temperature fluctuations, motion and diffusion can all result in a super-Poisson distribution resulting in $\sigma^2 > \mu$ (Teich & Saleh, 1988; Chen *et al.*, 1999). Most important for this study is the fact that biological processes would also contribute to the super-Poisson behaviour because they would not predictably follow a Poisson distribution. However, to detect a biological source of variation, the sources of super-Poisson variations, listed above, in the instrument measurement system must be known. Therefore, the use of an internal control to monitor instrument-based fluctuations is required.

We used the coefficient of variation (CV), defined as the standard deviation (σ) divided by the mean (μ), as a model-independent measurement for most comparisons. CV has also been extensively used in the analysis of the performance of confocal imaging devices (Zucker & Price, 2001).

Results and discussion

The noise characteristics of the confocal microscope were first characterized using a model sample. The model sample was a buffered solution of NADH set to be in the range of the fluorescence signal from isolated myocytes collected with the same photomultiplier tube (PMT) gain and laser amplitude. Histograms of fluorescence intensities as a function of [NADH] are presented in Fig. 1. Solid lines are theoretical curves of Poisson distributions for given mean intensities. The solution distributions are slightly broader than simple Poisson distributions at all concentrations studied, suggesting a super-Poisson condition even in the absence of a cell. As mentioned above, the super-Poisson behaviour is probably the result of fluctuation of the light source or mechanical noise sources under these control conditions. These data demonstrate the need for determining instrumental noise in analysing super-Poisson behaviour of intact cells.

The fluorescence amplitude of NADH was also altered by varying the temperature between 24 and 32 °C. Temperature quenching of the NADH fluorescence was found to be approximately 2% per degree Celsius. The CV values plotted as a function of fluorescence intensity for the temperature and [NADH] data sets are presented in Fig. 2. Both the temperature

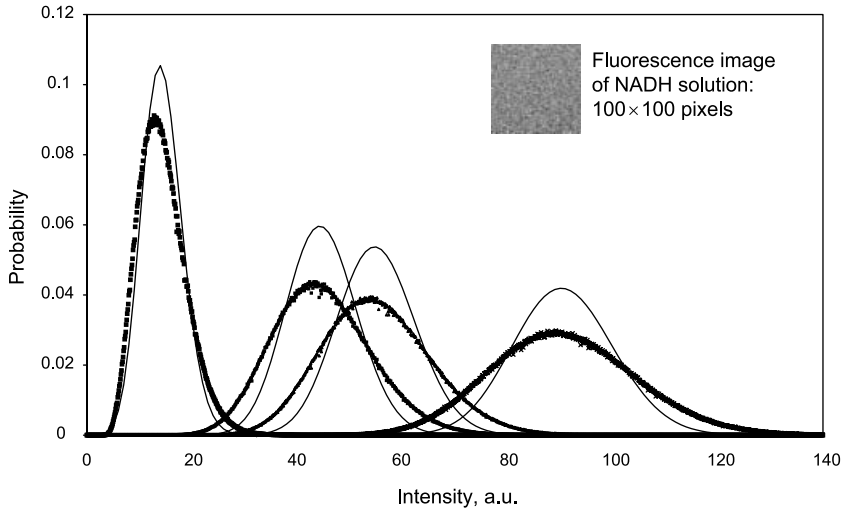

Fig. 1. Fluorescence intensity histograms for NADH solutions ([NADH] = 1.3×10^{-4}, 6.4×10^{-4}, 8.0×10^{-4} and 1.6×10^{-3} M), $T = 25$ °C. Dots – experimental data, solid lines – theoretical Poisson distributions for the experimental mean. Probability is the number of pixels with given fluorescence intensity divided by the total number of pixels (100 pixels × 100 pixels × 350 images).

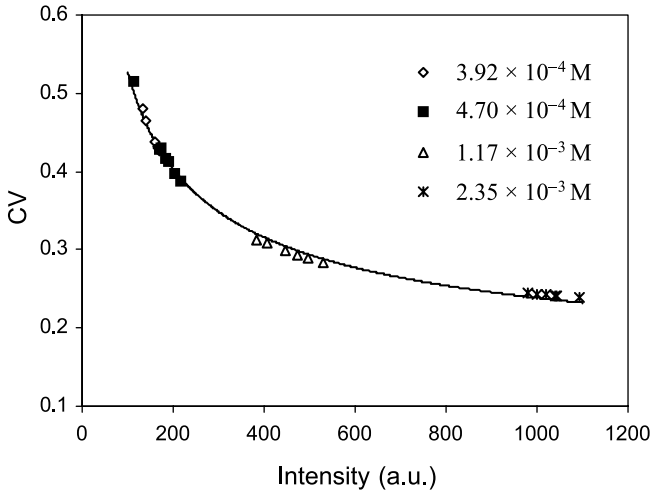

Fig. 2. Effect of [NADH] and temperature on the coefficient of variation. Each symbol represents the given [NADH] presented in the legend. Each [NADH] is presented at six different temperatures, 24, 26, 28, 30, 32 and 34 °C with the coefficient of variation decreasing with increasing temperature. The temperature variation of the NADH amplitude apparently falls on the same curve with the [NADH] data. The solid line is drawn to guide the eye.

(i.e. constant [NADH]) and [NADH] data fall on the same line. The data suggest that the fluctuation of the NADH signal is dominated by the instrument sampling processes and not by temperature-sensitive processes such as diffusion or alterations of the NADH molecule (i.e. potential self-association of NADH molecules).

Owing to the presence of a super-Poisson distribution in NADH fluorescence under control conditions, an experimental scheme for analysing the fluorescence fluctuations in cardiac myocytes was devised using a true internal standard. To accomplish this task, the cardiac myocytes were perfused with a media that contained an NADH solution generating a similar signal as the cell. To ensure that the extracellular NADH was not contributing to the cellular signal, the cellular NADH signal was monitored before and after the addition of NADH to the bath. In general, the bath NADH signal contributed ≤ 5% to the cellular signal under these conditions and was considered insignificant for this analysis. The exclusion of the solution NADH signal in the cell was due to maintaining the sensitive region of the sampling within the cell, as a result of the confocal point spread function, and the exclusion of extracellular space between the cell and cover-slip by the attachment process.

Single voxels or regions of interest were analysed in the cell and compared with a similar volume in the bath. An example from one of these studies is presented in Fig. 3. The top picture (Fig. 3A) is a confocal NADH fluorescence image of an entire resting rabbit myocyte without NADH in the bath to enhance the image contrast for this demonstration. Marked on this image are examples of the two reduced field of view images that were selected for the time course series, one in the bath and one in the cell. In Fig. 3(B) is a single voxel time course from the cellular image set along with an image (i) of the mean NADH fluorescence of this data set (100 pixels × 50 pixels × 600 images). A time course for a single voxel in the bath is presented in Fig. 3(C) alone with its mean amplitude image (iii). In the cell the NADH signal decreased as a result of UV photolysis of the NADH (Combs & Balaban, 2001). This was not observed in the bath (Fig. 3C) because it was being continually renewed by the perfusion with the NADH-containing media. A smoothed exponential decay was used to model the cellular data to compensate for the balance between photolysis and metabolism, as shown by the solid line in the time course data. This fitted exponential curve was then used to detrend the cell data by subtraction, leaving only the high-frequency fluctuation data. After this detrending procedure, the CV was calculated and is presented as an image for both the cell (ii) and bath (iv) data. Some 'structure' is still present in the CV image tracking the

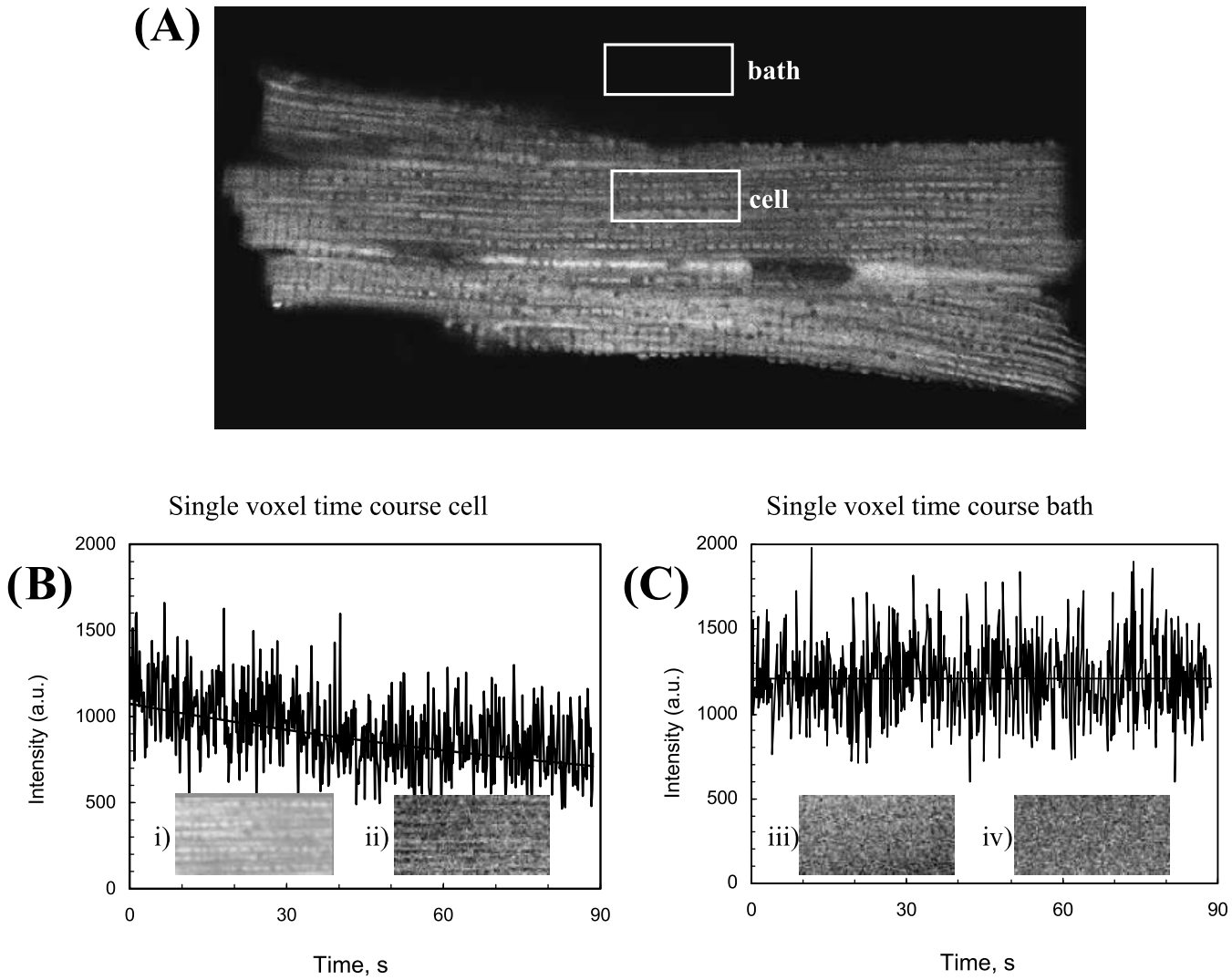

Fig. 3. NADH fluorescence time courses of bath and isolated cardiac myocyte. (A) NADH fluorescence image of an intact myocyte. Two regions are indicated (bath and cell) that represent the reduced field-of-view images that we simultaneously scanned to collect the time series data. (B) Time course of a single voxel in the cell. (C) Time course of single voxel in the bath image. The image inserts are: the average magnitude image of the entire cell time series (i) and the CV distribution of the individual voxels (ii), the average magnitude image of the entire bath time series (iii) and the CV distribution of the individual voxels (iv). The bath [NADH] was 9.2×10^{-4} M.

amplitude variation in the image. This correlation is expected because the CV decreases with increasing amplitude (see Fig. 2). However, it is apparent from the fluctuations in the time courses as well as the CV images that the bath signal and cellular data were, qualitatively, very similar.

Using this approach, we collected a time series for myocyte and internal control at different temperatures to generate a better dynamic range in the mean amplitude as well as, potentially, any biological processes. The temperature varied from 25 to 37 °C. After detrending the cell data and normalizing both the cell and the control data we calculated the CV for individual voxels in the bath and cell. The CV data for individual voxels as a function of the mean amplitude are presented in Fig. 4. The four discrete bands in the bath data are from the four temperatures (24, 31, 33 and 35 °C) used in this study, whereas the cellular NADH signal was, naturally, more dispersed. We found that CV in the both data sets are strongly dependent on the fluorescence. The cellular and bath CV were essentially identical at the same intensity values, suggesting that the instrument noise was dominating the variation detected. This was confirmed by increasing the dynamic range of NADH signals in the bath by changing bath [NADH] in addition to temperature. These data are summarized in Fig. 5, where the CV and intensities are plotted after averaging the entire image frame voxels for each time course to simplify the presentation. No significant difference was observed for

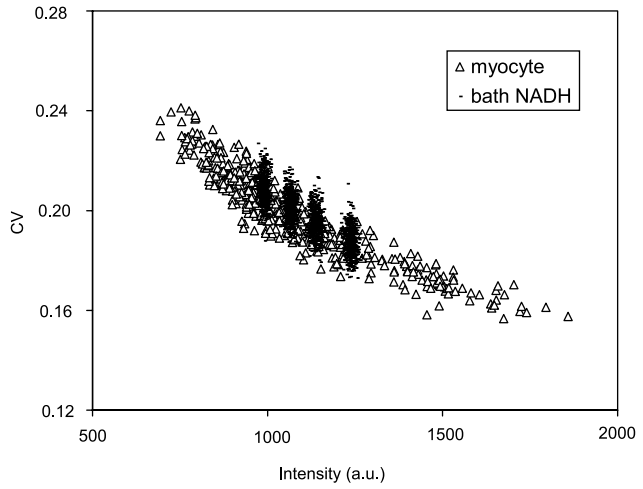

Fig. 4. Coefficient of variation vs. fluorescence intensity calculated for the single pixels in the bath and myocyte. The myocyte data plotted were for a single temperature at 24 °C. The bath data are ploted at three temperatures to improve the dynamic range in the presentation. The bath temperatures plotted are 24, 31, 33 and 35 °C. Lower temperatures resulted in higher NADH fluorescence signal intensity. The temperature dependence of the myocyte fluorescence was omitted to simplify the presentation.

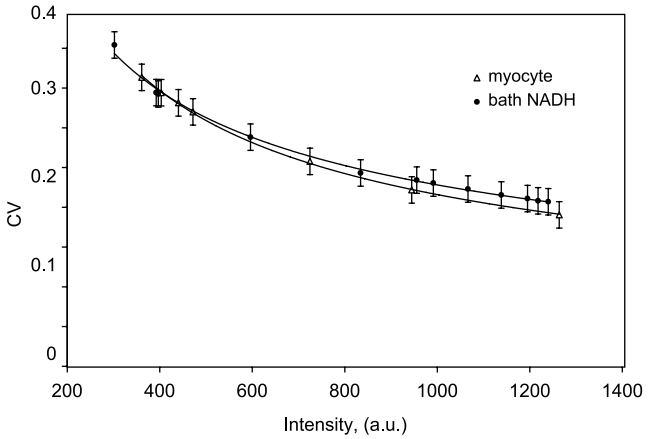

Fig. 5. Summary of NADH fluorescence CV in the isolated myocyte and bath. These summary data were derived by averaging the CV and amplitude data over the entire image of the cell or bath. Dynamic range in the amplitude data was generated by varying temperature and the concentration of NADH in the bath. Error bars represent the SD ($n = 60$). Solid lines are drawn to guide the eye.

these data sets in a paired t-test ($P > 0.05$) between the cell and bath image variations. Varying the sampling rate from 30 to 500 ms × frame^{-1} had no effect on this comparison.

The sensitivity of this measure to biological variations was estimated by evaluating the experimentally derived cellular CV histograms and determining what increase in CV would be required to reach statistical significance near the mean intensity observed in the cell. We found that the CV of a putative biological

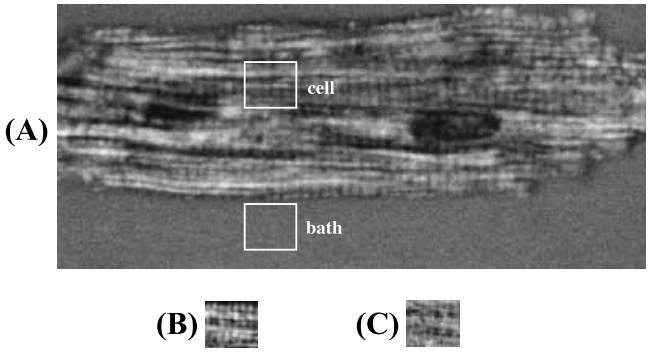

Fig. 6. NADH-fluorescence image of the living cardiac myocyte perfused with NADH solution taken with two-photon excitation confocal microscopy. (A) Whole cell image with NADH in solution with examples of reduced field of views used for time course image collection. (B) Average magnitude image of cell time course data. (C) Individual pixel CV image of cell data calculated from a time series.

process would require an excess fluctuation of $\Delta CV = 0.04$ in order to be detected over the background noise. This value of ΔCV corresponds to a sensitivity and specificity of 95%.

Both Fourier analysis and correlation analysis were performed to characterize further the NADH fluorescence time courses. Fourier analysis of time courses revealed no coherent spectral components. Pearson's correlation coefficient (ρ) was calculated across the time series in every neighbouring pixel. This coefficient measures the strength of the linear relationship between two variables, and can have from −1.0 (perfect negative correlation) to 1.0 (perfect positive correlation); $\rho = 0.0$ corresponds no correlation. We obtained a maximum correlation coefficient of 0.16 both in the cell image and the NADH in the bath analysing 100 pixels × 50 pixels × 600 images in both compartments. Because both the cell and the bath data revealed the same ρ value, it is likely that any correlation of the fluorescence signal in different parts of the cell is not significantly different from the background, and any existing correlation is probably due to systematic variations in sampling and processing of the data.

For comparative purposes, two-photon fluorescence time series were collected. The advantage of the multiphoton system over the usual confocal microscope is further selection of cellular NADH signal sources due to the lack of out-of-plane NADH excitation. However, the overall point-spread function is slightly less specific (Min Gu & Sheppard, 1995), whereas the squared dependence on the excitation light intensity may result in the laser fluctuations having a more significant effect on the observed noise. A whole cell NADH image is shown in Fig. 6(A) with NADH in the bath to illustrate the use of the internal standard. The reduced field-of-view (48 × 42 pixels) cell images are as shown as the mean (Fig. 6B) and CV (Fig. 6C). Two hundred reduced field-of-view images of living cardiac myocyte were acquired at 300-ms intervals for each time course. We obtained the lower CV values in the two-photon system

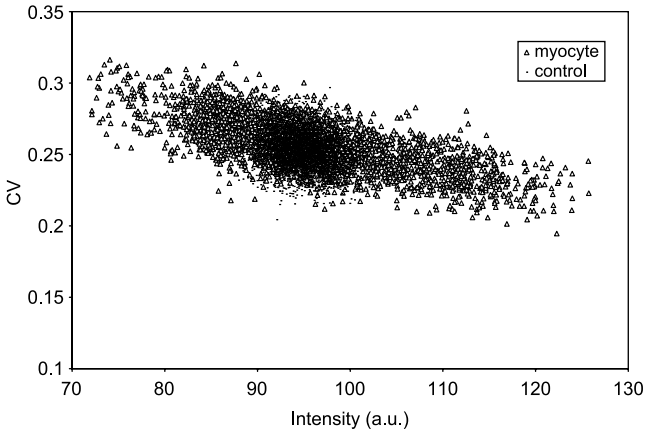

Fig. 7. Coefficient of variation of NADH fluorescence, in the two-photon excitation scheme, for isolated myocyte and in the free solution vs. mean NADH signal.

when compared with the same intensity values in the confocal instrument. These data suggest that the two-photon system had less instrumental noise than the confocal system. However, direct comparison of the CV values between the bath and cellular NADH signal demonstrated no significant difference in paired experiments ($P > 0.05$) (Fig. 7). These data are consistent with the suggestion that the instrument noise is still far greater than biological variations even in a dual-photon excitation instrument.

It is interesting to consider why we did not observe a systematic 'flickering' of the NADH signal in these cells in contrast to prior publications. Duchen *et al.* (1998) observed the regional fluctuations in the mitochondrial membrane potential of cardiac cells loaded with tetra-methyl rodamine-ethyl ester (TMRE). We have also observed these types of fluctuations in mitochondrial NADH in rabbit myocytes loaded with TMRE after extensive imaging experiments (i.e. long exposures to laser light). Thus, in our hands, the fluctuations might be induced by the TMRE–light interactions. It is also possible that our preparation did not have the Ca^{2+} sparks correlated with the regional mitochondrial membrane potential depolarization (Duchen *et al.*, 1998), because no measurements of regional cytosolic Ca^{2+} were made in the current studies. In the studies of Romashko *et al.* (1998) the fluctuations in flavine adenine dinucleotide (FAD) fluorescence was observed only after substrate deprivation. We did not attempt to repeat these experimental conditions in the current study.

Conclusions

NADH fluorescence fluctuations in living cardiac myocytes are dominated by the fundamental shot noise of the measurement and some apparently Gaussian noise sources in commercially available imaging systems. These data suggest that biological processes do not significantly influence the fluctuation of NADH fluorescence signals in resting cardiac myocytes using standard single-photon and two-photon approaches.

References

Chacon, E., Reece, J.M., Nieminen, A.L., Zahrebelski, G., Herman, B. & Lemasters, J.J. (1994) Distribution of electrical potential, pH, free Ca^{2+}, and volume inside cultured adult rabbit cardiac myocytes during chemical hypoxia: a multiparameter digitized confocal microscopic study. *Biophys. J.* **66**, 942–952.

Chen, Y., Muller, J.D., So, P.T. & Gratton, E. (1999) The photon counting histogram in fluorescence fluctuation spectroscopy. *Biophys. J.* **77**, 553–567.

Combs, C.A. & Balaban, R.S. (2001) Direct imaging of dehydrogenase activity within living cells using enzyme-dependent fluorescence recovery after photobleaching (ED-FRAP). *Biophys. J.* **80**, 2018–2028.

Duchen, M.R., Leyssens, A. & Crompton, M. (1998) Transient mitochondrial depolarizations reflect focal sarcoplasmic reticular calcium release in single rat cardiomyocytes. *J. Cell Biol.* **142**, 975–988.

Estabrook, R.W. (1962) Fluorometric measurements of reduced pyridine nucleotide in cellular and subcellular particles. *Anal. Biochem.* **4**, 231–245.

Huang, H., Dong, C.Y., Kwon, H.S., Sutin, J.D., Kamm, R.D. & So, P.T. (2002) Three-dimensional cellular deformation analysis with a two-photon magnetic manipulator workstation. *Biophys. J.* **82**, 2211–2223.

Klingenberg, M., Slenchzka, W. & Ritt, E. (1959) Verfleichende Biochemie de Pyridinnucleotid-Systeme in Mitochondrien verschiedener Organe. *Biochemische Z.* **332**, 47–66.

Mandel, L. & Wolf, E. (1995) *Optical Coherence and Quantum Optics.* Cambridge University Press, New York, NY.

Min Gu & Sheppard, C.J. (1995) Comparision of three-dimentional imaging properties between two-photon and single-photon fluorescence microscopy. *J. Microsc.* **177**, 128–137.

O'Rourke, B., Ramza, B.M., Romashko, D.N. & Marban, E. (1995) Metabolic oscillations in heart cells. *Adv. Exp. Med.* **382**, 165–174.

Romashko, D.N., Marban, E. & Rourke, B. (1998) Subcellular metabolic transients and mitochondrial redox waves in heart cells. *Proc. Natl Acad. Sci. USA*, **95**, 1618–1623.

Teich, M.C. & Saleh, B.E.A. (1988) Photon bunching and antibunching. *Progress in Optics* (ed. by E. Wolf), pp. 1–104. North-Holland Publishing Co, Amsterdam, The Netherlands.

Territo, P.R., Mootha, V.K., French, S.A. & Balaban, R.S. (2000) Ca (2+) activation of heart mitochondrial oxidative phosphorylation: role of F0/F1ATPase. *Am. J. Physiol.* **278**, c423–c435.

Wakita, M., Nishimura, G. & Tamura, M. (1995) Some characteristics of the fluorescence lifetime of reduced pyridine nucleotides in isolated mitochondria, isolated hepatocytes, and perfused rat liver in situ. *J. Biochem. (Tokyo)*, **118**, 1151–1160.

Zucker, R.M. & Price, O.T. (2001) Statistical evaluation of confocal microscopy images. *Cytometry*, **44**, 295–308.